nature COMMUNICATIONS

ARTICLE

Received 2 Dec 2014 | Accepted 29 Jan 2015 | Published 6 Mar 2015

DOI: 10.1038/ncomms7449

CCM-3/STRIPAK promotes seamless tube extension through endocytic recycling

Benjamin Lant[1], Bin Yu[1], Marilyn Goudreault[2], Doug Holmyard[2], James D.R. Knight[2], Peter Xu[3], Linda Zhao[1], Kelly Chin[1], Evan Wallace[1,3], Mei Zhen[2,3], Anne-Claude Gingras[2,3] & W Brent Derry[1,3]

The mechanisms governing apical membrane assembly during biological tube development are poorly understood. Here, we show that extension of the *C. elegans* excretory canal requires cerebral cavernous malformation 3 (CCM-3), independent of the CCM1 orthologue KRI-1. Loss of *ccm-3* causes canal truncations and aggregations of canaliculular vesicles, which form ectopic lumen (cysts). We show that CCM-3 localizes to the apical membrane, and in cooperation with GCK-1 and STRIPAK, promotes CDC-42 signalling, Golgi stability and endocytic recycling. We propose that endocytic recycling is mediated through the CDC-42-binding kinase MRCK-1, which interacts physically with CCM-3–STRIPAK. We further show canal membrane integrity to be dependent on the exocyst complex and the actin cytoskeleton. This work reveals novel *in vivo* roles of CCM-3 · STRIPAK in regulating tube extension and membrane integrity through small GTPase signalling and vesicle dynamics, which may help explain the severity of *CCM3* mutations in patients.

[1] Developmental and Stem Cell Biology Program, The Hospital for Sick Children, Peter Gilgan Centre for Research and Learning, 686 Bay Street, Toronto, Ontario, Canada M5G 0A4. [2] Lunenfeld-Tanenbaum Research Institute at Mount Sinai Hospital, 600 University Avenue, Toronto, Ontario, Canada M5G 1X5. [3] Department of Molecular Genetics, University of Toronto, 1 King's College Circle, Toronto, Ontario, Canada M5S 1A8. Correspondence and requests for materials should be addressed to W.B.D. (email: brent.derry@sickkids.ca).

Multicellular organisms contain myriad biological tubes that transport gases and fluids within organs and throughout the body. These tubes can develop through a variety of mechanisms, such as wrapping, cavitation and cell hollowing[1,2]. The mechanism of lumen formation, and regulation of tube diameter, is dependent on whether the tube is multicellular, autocellular or seamless. Seamless tubes are unicellular, do not have junctions and form by the process of cell hollowing[2]. Proper control of tube length and diameter is of fundamental importance during development, and defects can lead to pathologies, such as polycystic kidney disease and cerebral cavernous malformations (CCMs)[3,4]. Genetically tractable organisms (for example, the fruit fly *Drosophila melanogaster* and the nematode *Caenorhabditis elegans*) have revealed conserved mechanisms by which biological tubes develop and how their integrity is maintained[1,5,6].

The excretory canal is a seamless unicellular tube that maintains osmotic balance and ion levels in *C. elegans*[6,7]. Created in the embryo, the excretory cell projects two arms dorsolaterally until they reach the hypodermis, where they bifurcate and extend bi-directionally along the anterior/posterior axis, forming two long canals (Fig. 1a). As seen in a cross-section (Fig. 1b), canals are comprised of a basal (outer) membrane, a cytoplasmic region containing canalicular vesicles (CVs), organelles (endoplasmic reticulum (ER), Golgi and mitochondria), and an apical (inner) membrane that envelops the lumen. During its post-embryonic extension phase, actin-based projections stimulate outgrowth of the canal tip causing the excretory canal to undergo marked morphological changes[6]. It is thought that lumen formation and extension of the apical (luminal) membrane is the driving force of tubulogenesis, but how membrane is added during this growth phase is presently not well understood. The canals of lumen defective mutants do not extend and show accumulation and hyperfusion of CVs in the cytoplasmic space, which reveals important links between these membrane sources and canal morphology[8,9].

The current model of excretory canal development combines coalescence and fusion of vacuoles, activity of ion channels and aquaporins, cytoskeletal rearrangements and endocytic trafficking[8–10]. Endosomes, particularly through the slow recycling pathway, are critically important for facilitating plasma membrane building and subsequent maintenance. The *trans*-Golgi network (TGN) communicates with recycling endosomes (REs), providing secretory vesicles that contain proteins and lipids necessary for membrane building[11]. Endosomes sort the material and bud new vesicular carriers, which travel to and dock (with the aid of exocyst complexes) at the plasma membrane to unload their cargo. Surface material from the membrane is transported via endocytosis to endosomes, which sort and package the materials and membrane for return to the TGN. In this way, the endosomes and Golgi form a co-dependent relationship that sustains both the shape and function of the TGN and biogenesis of the TGN-derived vesicles, while promoting plasma membrane assembly and maintenance[11]. The small GTPase CDC-42 has been strongly implicated in regulating vesicle trafficking to and from Golgi[12–14].

Changes in the levels of signalling and structural proteins lead to defects in excretory canals. For example, loss-of-function mutations in the CDC-42 guanine nucleotide-exchange factor EXC-5 causes formation of large cysts in the apical membrane. In contrast, overexpression of EXC-5 causes canal truncations that arise through defects in the basolateral membrane[15]. Likewise, loss of the cytoskeletal linker Ezrin Radixin and Moesin family orthologue ERM-1 results in canal truncation and cyst formation, whereas overexpression causes severely widened lumen and cytoplasmic trailing at the distal tips[8]. Hence, maintaining the proper balance of small GTPase activity and cytoskeletal protein levels is critical for coordinating lumen formation and subsequent basolateral membrane addition during seamless tube extension.

CCM is a neurovascular disease that can arise in an autosomal dominant manner (familial) or sporadically by unknown mechanisms[16]. Both familial and sporadic CCM are characterized by defects in brain capillaries that develop into enlarged 'mulberry-like' cysts (that is, clustered, fluid-filled, aberrations in the plasma membrane). Defective cell–cell junctions in these lesions cause blood to leak into the brain, leading to symptoms such as headaches, seizures and stroke in the most severe cases[16]. Three causative genes for familial CCM have been identified, which encode distinct scaffold proteins KRIT1 (*CCM1*), malcavernin (*CCM2*) and PDCD10 (*CCM3*)[17–21]. Loss of the *CCM1* gene, the most common genetic lesion in familial CCM, results in hyperactivation of RhoA and the Rho-activated kinase (ROCK), which culminates in stress fibre formation and compromised cell–cell junctions[22]. Although the three CCM proteins can form a ternary complex[23], recent studies indicate that the majority of cellular CCM3 resides in the striatin interacting phosphatase and kinase complex (STRIPAK) and that CCM3 functions independently of CCM1 and CCM2 (refs 24–28). Critically, patients with mutations in the *CCM3* gene have an earlier onset of disease, often during childhood, and more severe neurovascular defects[29], supporting the idea that CCM3 may act by a mechanism that is distinct from CCM1 and CCM2.

We show here that the *C. elegans* CCM3/PDCD10 orthologue CCM-3 and its binding partners, germinal centre kinase III (GCK-1) and striatin (CASH-1) promote extension of excretory canals during post-embryonic development. Furthermore, CCM-3 and GCK-1 localize to the apical canal membrane, and their ablation causes severe canal truncation and cyst formation. We find that CCM-3 functions in a cell-autonomous manner to promote CDC-42 signalling and RE integrity, independent of the CCM1/KRIT1 orthologue KRI-1. Using transmission electron microscopy (TEM) we show that *ccm-3* loss-of-function mutants have defects in both basolateral and apical canal membranes. Apical defects, caused by dysregulated CV dynamics, result in formation of fluid-filled ectopic lumens (cysts) that resemble the 'mulberry-like' lesions of human CCM. These studies reveal a novel *in vivo* mechanism of action for CCM-3 as part of STRIPAK, which may help explain the more aggressive nature of this disease in patients harbouring mutations in the *CCM3* gene.

Results

Loss of CCM-3 affects excretory canal morphology. To investigate the biological function of *CCM3* in a genetically tractable multicellular organism, we identified the *C. elegans* orthologue *C14A4.11* (henceforth referred to as *ccm-3*), which encodes a protein of 215 amino acids that is 38% homologous to the mammalian protein[30]. To determine the expression pattern of CCM-3, we obtained a transgenic strain (BC13892) that contains a multicopy array expressing a transcriptional green fluorescent protein (GFP) reporter using 2,995 bp of the *ccm-3* promoter[31]. Strong GFP signal was detected in the excretory canals, vulva and intestine (Fig. 1c). Using the same promoter we generated a single-copy integrant expressing a CCM-3::GFP fusion protein and observed localization along luminal membranes of the intestine, pharynx and germline that recapitulated the expression pattern of the transcriptional reporter in all tissues except the excretory canals (Supplementary Fig. 1a–c). We suspect that endogenous CCM-3 is maintained at low levels in the canal owing to its toxic effects when overexpressed (see below). Using a canal-specific promoter (*exc-9*) we found that a CCM-3::GFP

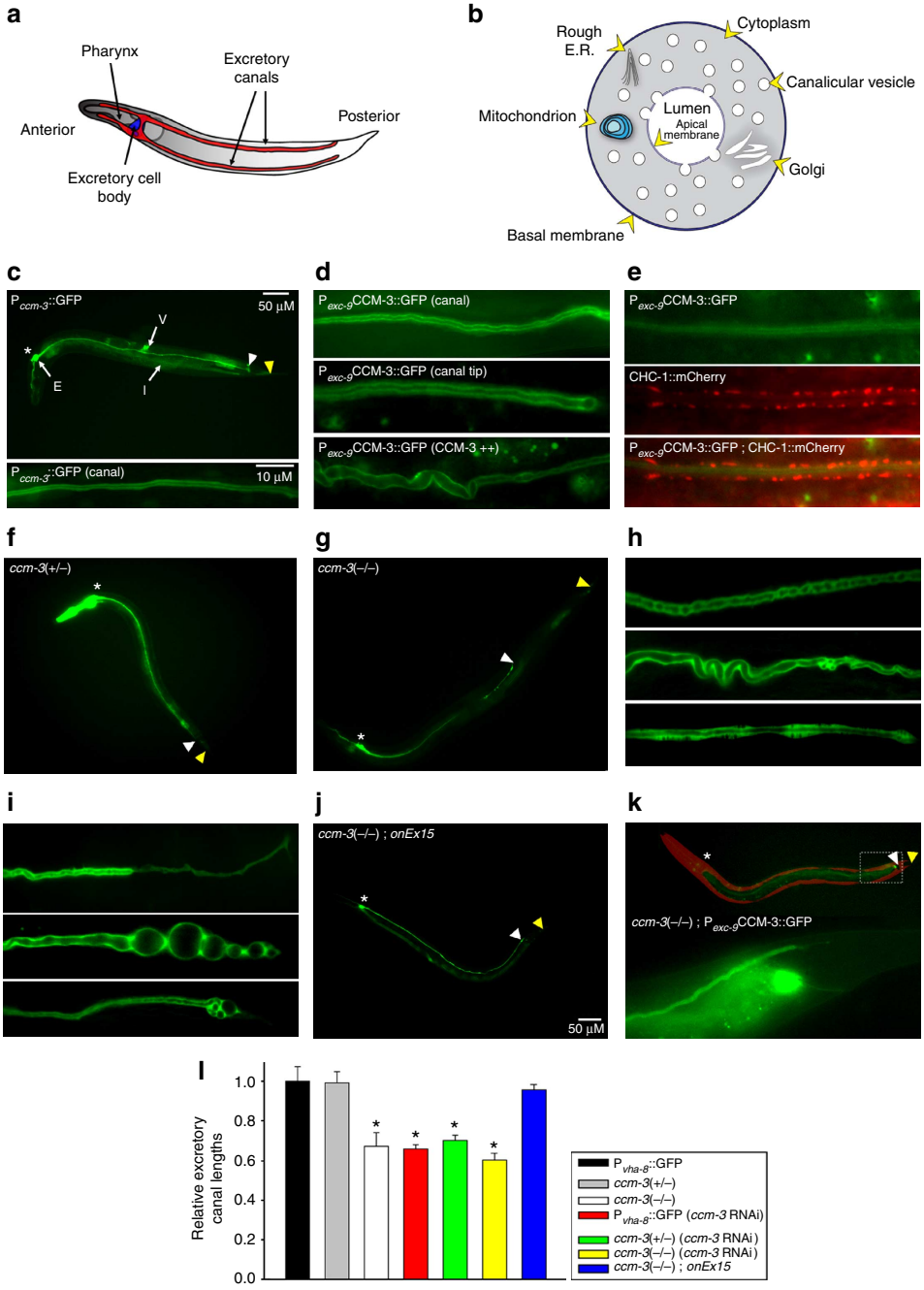

Figure 1 | Loss of *ccm-3* affects canal growth. (**a**) *C. elegans* excretory canals connect below the posterior bulb of the pharynx, extending two arms in anterior and posterior directions that create a distinctive 'H' shape. (**b**) Cross-sectional view of the canal depicts a basal membrane and cytoplasmic space in which membranous channels (canalicular vesicles, CVs) aggregate and fuse to form the lumen. Mitochondria, Golgi and ER are distributed along the length of wild-type canals. (**c**) The *ccm-3* promoter fused to GFP shows robust expression in the intestine (I), vulva (V) and excretory canals (E). (**d**) A canal-specific translational reporter indicates CCM-3 presence in the cytoplasm, and a strong enrichment at the apical membrane. Overexpression of CCM-3 causes a misshapen canal with a widened lumen (bottom panel). (**e**) Apical enrichment is confirmed through a co-localization with CHC-1 (a basolateral marker). While no canal defects (canal marked with P_{vha-8}::GFP) are evident with loss of one copy of *ccm-3* (**f**), loss of both copies causes canal truncations (**g**,**l**) and lumen defects (including cyst formation) along the length of the canal (**h**), and at the distal tip (**i**). Expression of CCM-3 from its endogenous promoter fully rescues canal truncations in *ccm-3*(−/−) (**j**,**l**), while expressing CCM-3 using the canal-specific *exc-9* promoter (indicated by the red signal of co-injection marker) rescued canals in *ccm-3*(−/−) to wild-type length (region marked by an inset box) (**k**,**l**). In addition, *ccm-3(RNAi)* causes truncation in the canal like the homozygous mutation (**l**). Asterisks denote location of the excretory cell (at the anterior/head of the worm), white and yellow arrowheads denote canal and total worm length, respectively. All canals are oriented from anterior (left) to posterior (right). **c** (top), **f**,**g**,**j** and **k** (top) are at ×100 magnification; **c** (bottom), **d**,**e**,**h**,**i** and **k** (bottom) are at ×630 magnification. Scale bars are indicated for whole worm and high-magnification canal sections in the first appropriate panel, and are modified only in panels where the magnification is different. Graph shows average ± s.e.m., $n \geq 60$, $^*P < 0.05$ versus control (Student's *t*-test).

translational reporter showed localization to the apical membrane (Fig. 1d), confirmed by co-expression of the canal-specific basolateral marker CHC-1::mCherry (Fig. 1e). Extra-chromosomal arrays often overexpress proteins in *C. elegans*[32]. We observed that transgenic animals with markedly brighter signal (likely due to an overexpression of CCM-3::GFP) coincided with canals possessing distinctly widened lumens (Fig. 1d—third panel). We also observed frequent (>50%) enrichment of CCM-3, displayed as bright spots and short trails at the tips of healthy extending canals (Supplementary Fig. 1d).

To assess the biological function of *ccm-3*, we examined the phenotype of a *ccm-3* deletion allele (*tm2806*). The *tm2806* allele is a 442-base deletion that removes the second and third exons, and part of the forth exon, of the *ccm-3* gene. This allele is predicted to generate a protein of 52 amino acids that is out of frame after amino-acid 25 and is likely a null allele since most of the N-terminal region required for interaction with its binding partner GCK-1 is removed[25,30] (see below). Homozygous *ccm-3(tm2806)* mutants are sterile and develop slower than wild-type (WT) animals. Given the importance of *CCM* genes in vascular development, we investigated a potential role for CCM-3 in excretory canals by introducing a canal-specific reporter ($P_{vha\text{-}8}$::GFP) into *ccm-3(tm2806)* mutants. While *ccm-3* heterozygotes (marked as '+/−') did not have defective canals (Fig. 1f), homozygous mutants (marked as '−/−') had canal truncations to ~65% of their WT lengths (Fig. 1g,l). Truncations in *ccm-3(−/−)* worms were observed as early as the L3 larval stage of development, and the severity progresses into the adult stage, indicating an important role for CCM-3 in continuous post-embryonic excretory canal development. In addition, the existing canals exhibited multiple defects, including discontiguous (unconnected) lumen (Fig. 1h, top panel), or otherwise ectopic lumen separate from the primary lumen, which were confirmed through Z-stack analysis. Also common was widening of the lumen, presence of cysts (Fig. 1h, middle panel) and swollen cytoplasmic vesicles (Fig. 1h, bottom panel) that perturb the basolateral membrane. At the distal tip, as well as long thin trails of cytoplasmic material (Fig. 1i, top panel), lumenal cysts were also readily observed (Fig. 1i, middle and bottom panels). These defects are present in ~95% of *ccm-3(−/−)* mutants, with cysts in over 40% (Supplementary Table 1). Canal integrity worsens as the mutant animals age, taking the form of numerous fluid-filled bubble-like enlargements in the lumen (Fig. 1i, middle panel) and enlarged vesicles in the cytoplasm that severely distort the basolateral membrane. Introducing WT *ccm-3* under the control of its endogenous promoter rescued canal truncations and cysts in *ccm-3(−/−)* (Fig. 1j). Furthermore, ablation of *ccm-3* by RNA interference (RNAi) completely recapitulated canal truncations seen in *ccm-3(tm2806)* homozygotes (Fig. 1l).

To determine whether CCM-3 promotes canal extension by a cell-autonomous mechanism, we used the canal-specific translational reporter to express CCM-3 in *ccm-3(−/−)* worms. This rescued canal truncations and cysts (Fig. 1k), but not sterility, indicating that *ccm-3* acts in a cell-autonomous manner to promote canal extension and integrity. We observed CCM-3::GFP overexpression in ~20% of these transgenic worms, which caused defects such as severe canal truncations, expanded lumens and strong cystic profiles (Supplementary Fig. 1e). Overexpression did not, however, change the apical localization of CCM-3 (Supplementary Fig. 1f). Similar defects have been reported by overexpression of canal structural proteins[8,10].

The *C. elegans* genome contains homologues for two human CCM genes (*kri-1*/*CCM1* and *ccm-3*/*CCM3*). We previously identified a non-autonomous role for the CCM1 orthologue *kri-1* in promoting germline apoptosis[33]. No canal defects were observed in *kri-1* mutants (Supplementary Fig. 2a), supporting an emerging view that CCM3 has functions that are distinct from CCM1 and CCM2 (ref. 28). Using a KRI-1::GFP reporter (Supplementary Fig. 2b), previously shown to be expressed in the pharynx and intestine (Supplementary Fig. 2c,d)[33,34], we confirmed that *kri-1* is not detectably expressed in the excretory canals. Consistent with *ccm-3* and *kri-1* having distinct biological functions, we found that their co-ablation also results in synthetic lethality (Supplementary Fig. 2e).

GCK-1 interacts with CCM-3 and promotes canal extension. The C-terminal domains of each of the three GCKIII kinases (MST4, STK24 and STK25), the human orthologues of GCK-1, were previously shown to interact with the amino terminus of CCM3, and the critical residues required for contact are conserved in the worm proteins[30]. To determine whether worm CCM-3 and GCK-1 can also interact physically, we tagged these proteins with FLAG and GFP epitopes (respectively) and expressed them in HEK293T cells. Indeed, CCM-3 and GCK-1 physically interact, as shown by co-immunoprecipitation assays (Fig. 2a). Our canal-specific translational reporter for GCK-1 exhibited localization along the apical membrane, as well as the cytoplasm (Fig. 2b). Consistent with the biochemical data, we observed strong co-localization between GCK-1 and CCM-3 along the apical membrane of the canal (Fig. 2c).

Ablation of *gck-1* by mutation or RNAi caused similar canal truncations and cyst formation as observed in *ccm-3(−/−)* (Fig. 2e,f). Canal truncations in *gck-1(−/−)* were rescued by a *gck-1(+)* transgenic array expressed from its endogenous promoter (Fig. 2g,l). To determine whether its kinase activity is required for tube extension, we generated a transgenic strain expressing a mutant GCK-1 containing amino-acid substitutions (K62R and T186A) that render it catalytically inactive[35,36]. This kinase dead mutant failed to rescue canal truncations when expressed in *gck-1(−/−)* worms (Fig. 2h,l), supporting a catalytic role for GCK-1 in promoting canal elongation. To assess autonomy, and determine whether *gck-1* acts downstream of *ccm-3*, we injected the canal-specific mCherry::GCK-1 translational reporter into *gck-1(−/−)* and *ccm-3(−/−)* worms, which restored canals to normal lengths in both genetic backgrounds (Fig. 2i,j). Conversely, expression of CCM-3 could not rescue canal defects of *gck-1(−/−)* mutants (Fig. 2k). These results indicate that the kinase activity of GCK-1 is necessary for canal elongation, and that it functions genetically downstream of CCM-3.

CCM-3 affects CDC-42 activity and REs. Mammalian CCM1 and CCM2 proteins negatively regulate the small guanine nucleotide-exchange factor RhoA to maintain vascular integrity[22,37]. Whether small GTPases are regulated by CCM3 is less clear[37–39]. In the *C. elegans* excretory system, ablation of the CDC-42-activating guanine-exchange factor EXC-5 causes severe canal truncations and cyst formation, possibly through defects in endocytic recycling[10] (Fig. 3a). Loss of *rab-11*, a critical small GTP-binding protein that associates with REs and plays a key role in vesicle trafficking, causes canal truncations (Fig. 3b, top panel), cyst formation and discontiguous lumen (Fig. 3b, bottom panel) that resemble *ccm-3(−/−)* phenotypes. We therefore wished to address whether CCM-3 was implicated in the regulation of CDC-42. To do this, we monitored its localization using CDC-42::mCherry and its activation using GBDwsp-1::mCherry translational reporters[10]. In WT animals, these markers appear as punctate cytoplasmic bodies distributed along the length of canals (Fig. 3c–g; Supplementary Table 2). In *ccm-3(−/−)*, we observed a striking reduction in CDC-42 and activated CDC-42 puncta (Fig. 3c,d).

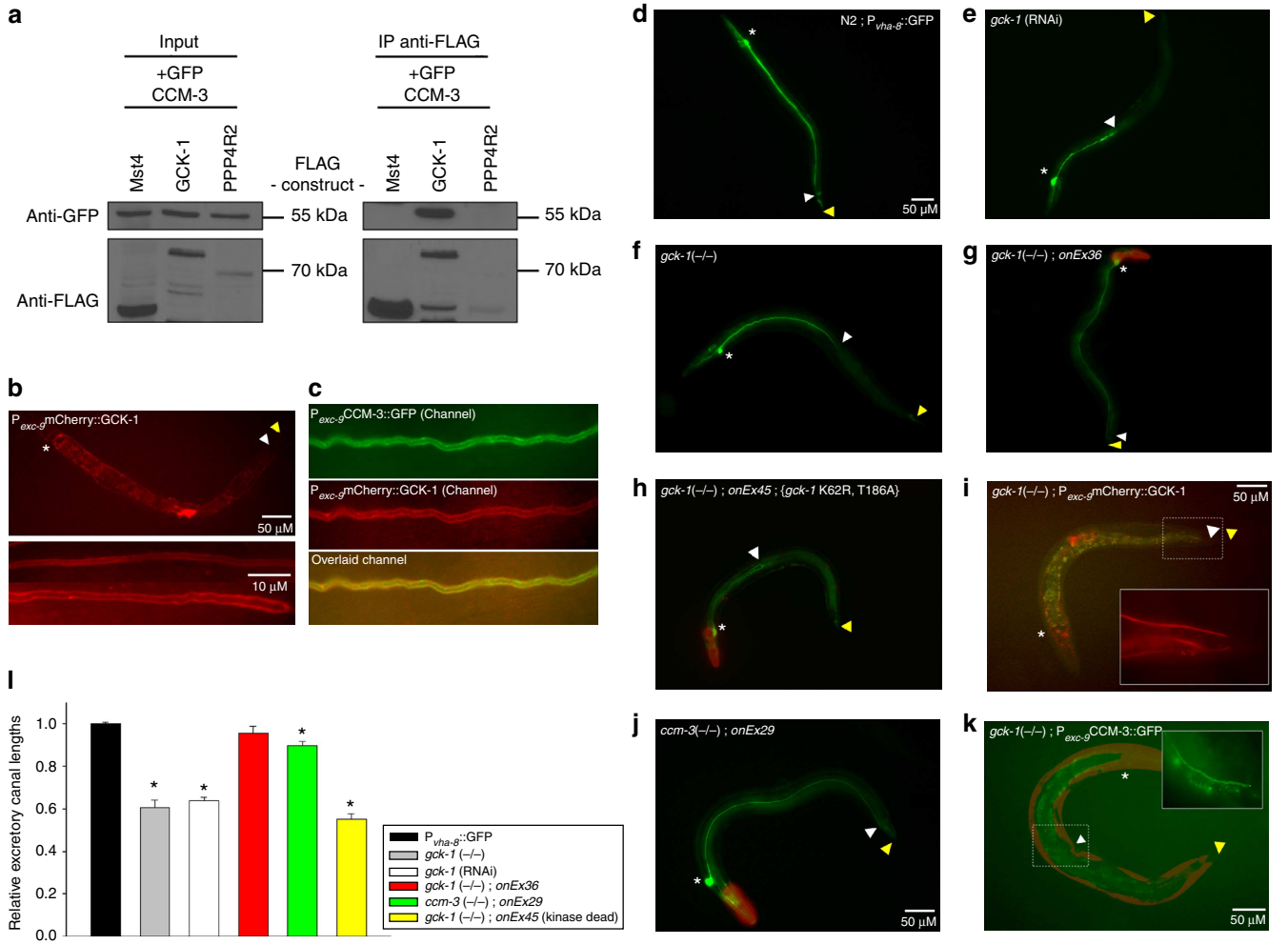

Figure 2 | CCM-3 promotes canal extension through GCK-1. (**a**) Co-immunoprecipitation of FLAG-tagged GCK-1 and GFP-tagged CCM-3 in HEK293T cells. Mst4 is the murine orthologue of GCK-1 that interacts with mammalian CCM3 ref. 30, but not *C. elegans* CCM-3. PPP4R2 is a human phosphatase-associated protein that does not interact with human STRIPAK and is used here as a negative control. (**b**) A translational reporter for GCK-1 indicates strong presence along the apical membrane and in the cytoplasm. (**c**) GCK-1 co-localizes with CCM-3 in the canal. (**d**) Canals in wild-type background extend to full length of the body, compared with truncations after cultivating wild-type worms on *gck-1(RNAi)* (**e**) or in *gck-1(−/−)* (**f**), which have canal truncations to ~60% of control lengths (**l**). Expression of wild-type GCK-1 (**g**) but not a kinase dead mutant (**h**) from its endogenous promoter (transgenic animals indicated by the red signal of co-injection marker in the pharynx) rescued truncated canals in *gck-1(−/−)*. Loss of GCK-1 was rescued by canal-specific GCK-1 overexpression (region marked by an inset box) (**i**), indicating cell autonomy. Overexpression of wild-type GCK-1 in *ccm-3(−/−)* rescued canals back to wild-type lengths (**j**,**l**), indicating that CCM-3 promotes canal extension through catalytically active GCK-1. CCM-3 overexpression, however, could not rescue loss of GCK-1 (region marked by an inset box) (**k**). Asterisks denote location of the excretory cell (at the anterior/head of the worm). White and yellow arrowheads denote canal and total worm length, respectively. All canals are oriented from anterior (left) to posterior (right). **b** (top), **d**–k are at ×100 magnification; **b** (bottom), **c** and insets are at ×630 magnification. Graph shows average ± s.e.m., $n \geq 20$, $^*P < 0.05$ from control (Student's *t*-test).

Because mammalian CDC-42 is required for endocytic trafficking, a process that is known to be critical for canal development[10], we asked whether CCM-3 affects early, late and/or RE markers. We introduced fluorescent markers of the Golgi (GRIP::mCherry), early endosome (RAB-5::mCherry) and RE (RAB-11::mCherry) into *ccm-3(−/−)* (Fig. 3a,e–g). Ablation of *ccm-3* did not affect early or late endosomes (RAB-7::mCherry), but caused a severe dispersal of Golgi (Fig. 3e,f; Supplementary Fig. 3e) and diminished RE reporter signals (Fig. 3g), which are normally distributed throughout the canal in WT animals[10]. The phenotypes in *ccm-3(−/−)* were phenocopied by RNAi (Supplementary Fig. 3), suggesting that CCM-3 promotes a CDC-42-dependent endocytic recycling process.

CCM-3 is required for membrane integrity. Canal truncations and cyst formation that occur in later stages of larval development of *ccm-3* mutants may indicate a breakdown of canal maintenance during its extension. To determine ultrastructural features of defective excretory canals in *ccm-3* mutants, we viewed serial cross-sections of canals using TEM. There were striking structural changes at both the basolateral and apical membranes in canals of *ccm-3(−/−)* compared with WT animals (Fig. 4a,b). Whereas WT canals are generally round with organized apical and basolateral membranes, *ccm-3(−/−)* showed distinctive projections off the basolateral membrane and enlarged lumen (Fig. 4b). While both rough ER and Golgi bodies were readily observed within the cytoplasm of WT canals (Fig. 4a), they were rarely observed in *ccm-3(−/−)* canals although mitochondria were observed in both (Fig. 4a,b; Supplementary Table 3). Indeed,

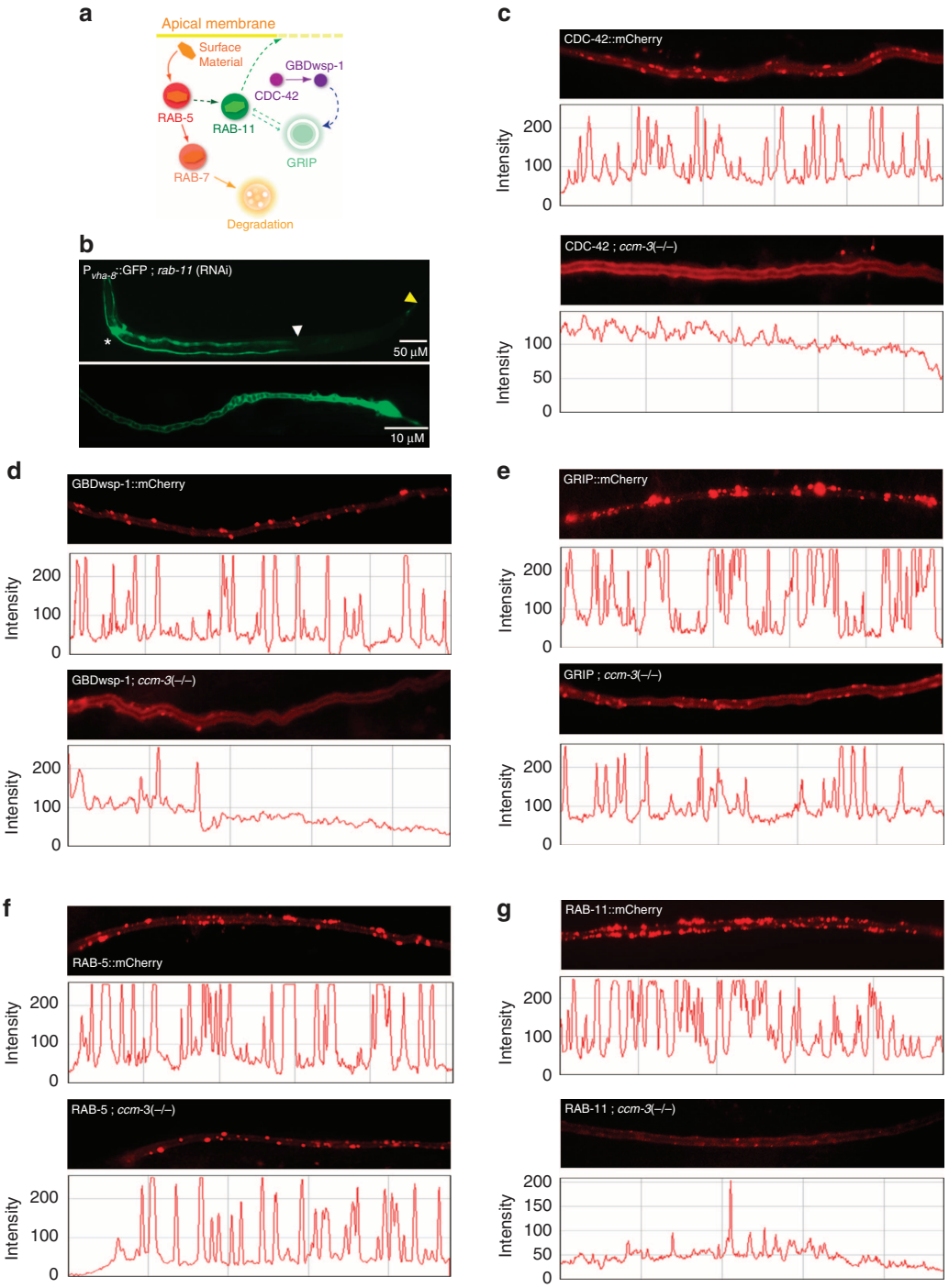

Figure 3 | CCM-3 promotes CDC-42 signalling and endocytic recycling. (**a**) Model of endocytic recycling in the excretory canal. Labels indicate vesicular compartments and signalling molecules studied with specific marker lines. Material is shuttled from the apical membrane into early endosomes (RAB-5). The path to degradation, via late endosomes (RAB-7), is marked with solid arrows. The path to material recycling linked to membrane growth through recycling endosomes (RAB-11), in contact with the *trans*-Golgi network (GRIP), and mediated by CDC-42 signalling (GBDwsp-1 indicates active CDC-42), is marked with dashed arrows. (**b**) The importance of recycling is shown through loss of *rab-11*, which causes canal truncation as well as significant lumenal defects and perturbations to the basolateral membrane (bottom panel). (**c**–**f**) Top panels show canal expression of the indicated mCherry-tagged proteins (forming punctuate bodies) in wild-type versus homozygous *ccm-3* mutants (bottom panel). Below canal images are fluorescence intensity traces along the respective canals, where peaks indicate puncta of the tagged marker protein. Presence of CDC-42 and its activated form (**c**,**d**) are severely reduced in the absence of *ccm-3*. Golgi bodies (represented by the GRIP::mCherry marker) (**e**) are also diminished, indicating that CCM-3 is required for Golgi presence (or stability) along canals. While loss of *ccm-3* does not affect distribution and abundance of RAB-5 (early endosomes) (**f**), the lack of intact Golgi may also affect endocytic recycling, as indicated by diminished RAB-11::mCherry (**g**) puncta. **b** (top) is at $\times 100$ magnification. **b** (bottom) and **c**–**g** show posterior regions of the canal at $\times 630$ magnification. All canals are oriented from anterior (left) to posterior (right).

while there were significant reductions in Golgi/ER even in the anterior-most sections, mitochondria were seen more frequently in *ccm-3* mutant worms (Supplementary Table 3), although this is likely due to a static number of mitochondria dispersed throughout a much shorter tube. Distinctively, *ccm-3(−/−)* canals contain more than double the number of CVs compared with WT (Fig. 4e). The increased CV number was accompanied by an increase in lumen diameter that led to a doubling of lumen volume (Fig. 4e). Loss of *ccm-3* appears to prevent normal CV incorporation into the lumen that drives canal development, similar to the dysregulation of cytoskeletal proteins (and organizers, such as ERM-1)[8,9]. Despite the shared phenotype of CV aggregation, loss of *ccm-3* did not change ERM-1 localization, nor could overexpression of ERM-1 rescue *ccm-3* mutant phenotypes (Supplementary Fig. 4), which suggests that CCM-3 may act independently of ERM-1.

During development, the canal contains beaded projections at intervals along its length called varicosities (Fig. 4c). These varicosities contain an abundance of cytoplasmic material and organelles that are thought to provide membrane and proteins for canal extension. Although there is an accumulation of cytoplasmic material in varicosities of WT worms, there is no change in CV abundance or lumen diameter. Hence, part of the cystic phenotype (ectopic lumen formation and cytoplasmic vesicle swelling) of *ccm-3* mutants is likely due to improper CV aggregation, which may be exacerbated by the addition of vesicles derived from fragmented Golgi (Fig. 4d). Many of these vesicles are expanded in size and can be up to four times the width of the uniform-sized WT CVs (Fig. 4f). Further, TEM images reveal hyper-aggregated CVs that apparently generate ectopic lumen (Fig. 4d, inset). This may result from the rate of vesicle fusion events exceeding that of endocytic recycling, as suggested by Kolotuev *et al.*[9]

To assess the progression of canal defects along its length, we sampled multiple short regions, at 50-μm intervals, with serial sections (Supplementary Fig. 5a). Canals in WT worms were uniform in shape, size and organelle content along their lengths (Supplementary Fig. 5b). In contrast, *ccm-3(−/−)* canals exhibited substantial basolateral membrane protrusions, as well as an expanded and progressively more damaged lumen towards the distal (posterior) tips (Supplementary Fig. 5c). In addition, rough ER and Golgi bodies were only observed in the anterior-most section of *ccm-3(−/−)* canals, and absent from the posterior sections (Supplementary Fig. 5c, top panel). This is consistent with our observations using the GRIP::mCherry Golgi marker (Fig. 3e). Therefore, canal defects in *ccm-3* mutants exhibit a progressively more severe phenotype towards their distal tips.

GCK-1/STRIPAK promotes canal elongation. In mammals the core STRIPAK complex is assembled via direct interactions between the striatin scaffold, protein phosphatase PP2A and CCM3, which recruits GCKIII class kinases[25]. Several other molecules of poorly characterized function also assemble on this well-defined core phosphatase and kinase module[25,40,41]. The *cash-1*, *farl-11*, *C30A5.3* and *C49H3.6* genes encode worm

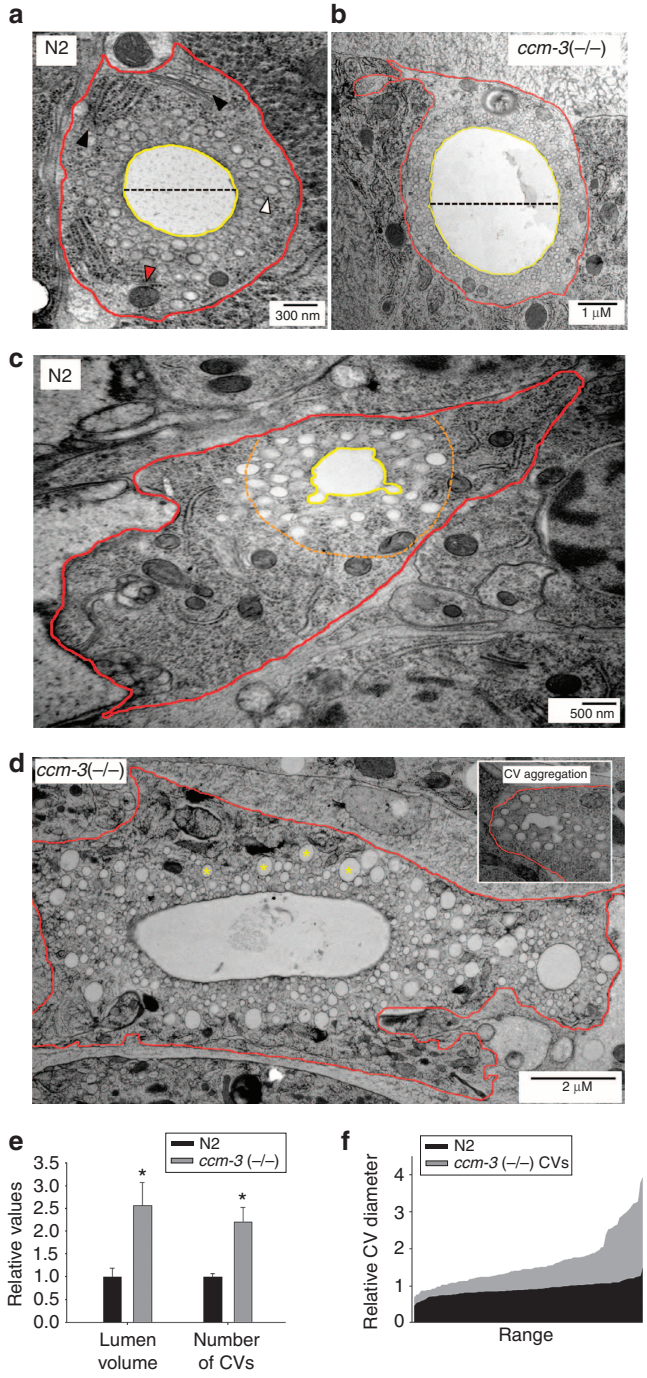

Figure 4 | *ccm-3* mutant canals have expanded lumen and increased canalicular vesicles. (**a**) Canals from wild-type worms display continuous and rounded basolateral membranes (marked in red) with similarly rounded apical/luminal (marked in yellow) membranes. In contrast, the *ccm-3* mutant canal (**b**) shows a projection from the basolateral membrane, along with an expanded lumen (lumen diameters indicated with a dashed line). Arrowheads in the control canal (**a**) indicate Golgi and rough endoplasmic reticulum (solid black), mitochondria (red) and CVs (white); there are no visible Golgi/ER structures in *ccm-3* mutant canals. (**c**) Developing canals often exhibit 'bulbs' of accumulated canal material (cytoplasm, organelles and so on) known as varicosities. Within these, the lumen size and number of CVs do not change. The dotted orange line indicates the approximate size of a standard N2 worm canal. (**d**) Heavily cystic canals (from *ccm-3* mutants) contain ectopic lumen (inset indicating nonspecific CV aggregation) and enlarged CVs (indicated by yellow asterisks). Quantification indicates that both lumen volume and number of CVs are doubled (**e**) (graph shows average ± s.e.m., $n=5$, $^*P<0.05$ (Student's *t*-test)) in *ccm-3* mutant canals. CV size show great variability in *ccm-3* mutant canals compared with wild-type controls (**f**) ($n=100$). All canal images were taken towards the anterior of the worm, within 100 μm of the excretory cell body at ×19,000 magnification (except **d**; ×6,500 magnification).

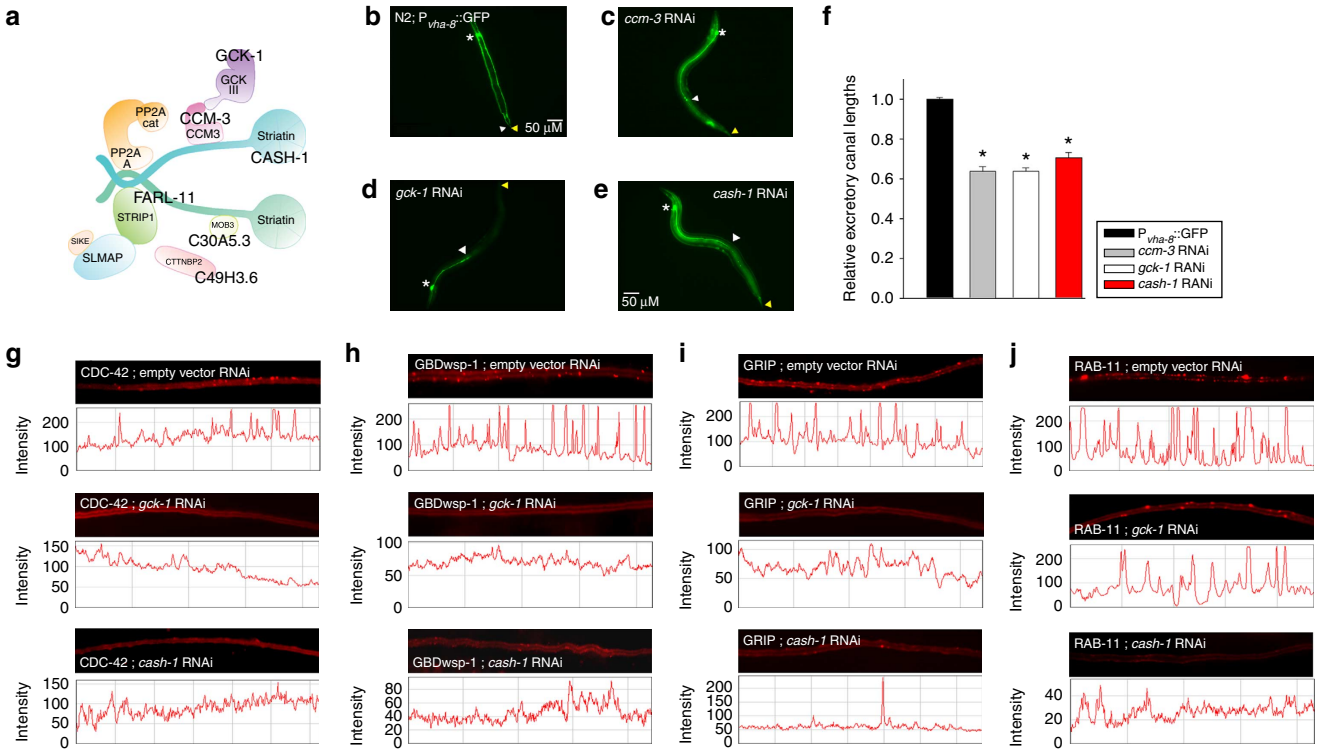

Figure 5 | STRIPAK promotes canal extension and endocytic recycling. (**a**) The STRIPAK complex is composed of multiple interacting proteins that are conserved in *C. elegans* (indicated in bold). Compared with N2 controls (**b**), ablation of core STRIPAK genes *ccm-3* (**c**), *gck-1* (**d**), the *C. elegans* striatin orthologue *cash-1* (**e**) and *farl-11*/STRIP1/2 caused similar canal truncations (**f**, Supplementary Table 4). (**g**–**j**) RNAi to empty vector (top), *gck-1*(middle) and *cash-1* (bottom), respectively. Ablation of STRIPAK components by RNAi atteunated CDC-42 signalling (**g**,**h**), as indicated by reduced puncta. The presence of Golgi (**i**) and recycling endosomes (**j**) were similarly reduced by ablation of *gck-1* and *cash-1*. Asterisks denote location of the excretory cell (at the anterior/head of the worm), white and yellow arrowheads denote canal and total worm length, respectively. **b**–**e** are at ×100 magnification; **g**–**j** are at ×630 magnification. All canals sections are taken from the same region, oriented from anterior (left) to posterior (right). Truncations range from ~30 to 40% from controls (**b**). Graph shows average ± s.e.m., $n \geq 20$, $^*P < 0.05$ from control (Student's *t*-test).

orthologues of striatin, STRIP1/2, MOB3 and CTTNBP2/NL, respectively (Fig. 5a; Supplementary Table 4)[40]. With the exception of MOB3 and CTTNBP2/NL, ablation of every component of the predicted *C. elegans* STRIPAK complex caused truncations in canals, similar to *ccm-3(−/−)* (Fig. 5b–f; Supplementary Table 4). We also asked whether ablating GCK-1 or other STRIPAK components affected endocytic recycling in a similar manner as CCM-3. In the absence of *gck-1* (Fig. 5g–j, middle panels) or *cash-1* (Fig. 5g–j, bottom panels) there was a drastic reduction in CDC-42, activated CDC-42, as well as reduced presence of Golgi and REs (Supplementary Table 2).

Given the reported similarity in loss of RAB-11 with a loss of the exocyst complex, which tethers vesicles arriving from the Golgi to the plasma membrane[42–44], we wondered whether the exocyst was also required for canal integrity. We introduced the *vha-8*::GFP canal marker in a strain carrying the *exoc-8(ok2523)* deletion allele and observed moderate canal truncations (Supplementary Fig. 6a,d), while loss of *ccm-3* in conjunction with *exoc-8* did not exacerbate these defects beyond truncations observed in *ccm-3* single mutants (Supplementary Fig. 6b,d). Despite a relatively moderate truncation effect, *exoc-8* mutants exhibited extremely strong cystic profiles (Supplementary Fig. 6c), in agreement with a recent report[45]. Along with apical cysts at the canal tip (Supplementary Fig. 6c, right panels), discontiguous lumen, enlarged cytoplasmic vesicles and perturbed basolateral membranes were frequently observed. It is possible, given the effect of CCM-3 on recycling components that EXOC-8 and CCM-3 cooperate to promote trafficking.

CDC-42 regulates canal length and Golgi/RE integrity. Following our observations of reduced CDC-42 presence with ablation of CCM-3 and other STRIPAK components, we asked whether CDC-42 was required for canal extension. Ablation of *cdc-42* by mutation or RNAi caused truncations and canal cyst formation similar to loss of *ccm-3* (Fig. 6a). Furthermore, ablation of *cdc-42* reduced Golgi and RE markers to a similar extent as loss of *ccm-3* (Fig. 6d–g, middle panels; Supplementary Table 2). To test the specificity of CDC-42 in promoting canal extension, we inhibited other small GTPases, *rho-1* (RhoA) and *chw-1* (RhoU/RhoV) by RNAi and observed no effects on WT canals (Supplementary Fig. 7a,b). Given the role of CCM3 (in its complex with CCM1 and CCM2) in repressing RhoA activity[4,22], we asked whether *rho-1* ablation could restore canal length or RE puncta in *ccm-3(−/−)*. Loss of *rho-1* had no discernable effect on canal length nor on RAB-11 puncta in *ccm-3(−/−)* worms (Supplementary Fig. 7c), positioning CDC-42 as the main Rho GTPase effector of the putative *C. elegans* CCM3–STRIPAK signalling pathway.

Activation of RhoA upon loss of CCM proteins leads to the formation of actin stress fibres[22]. Given the roles of actin in vesicular transport and TGN dynamics, we next asked whether increasing the pool of available actin could rescue loss of *ccm-3*. Introducing an extra-chromosomal array that overexpresses ACT-5::GFP into the *ccm-3(−/−)* worms caused a fourfold increase in full rescue (canal length >90%, relative body length) compared with *ccm-3(−/−)* (Supplementary Fig. 8). Interestingly, the number of RAB-11 puncta in rescued canals increased slightly (Supplementary Table 2), suggesting

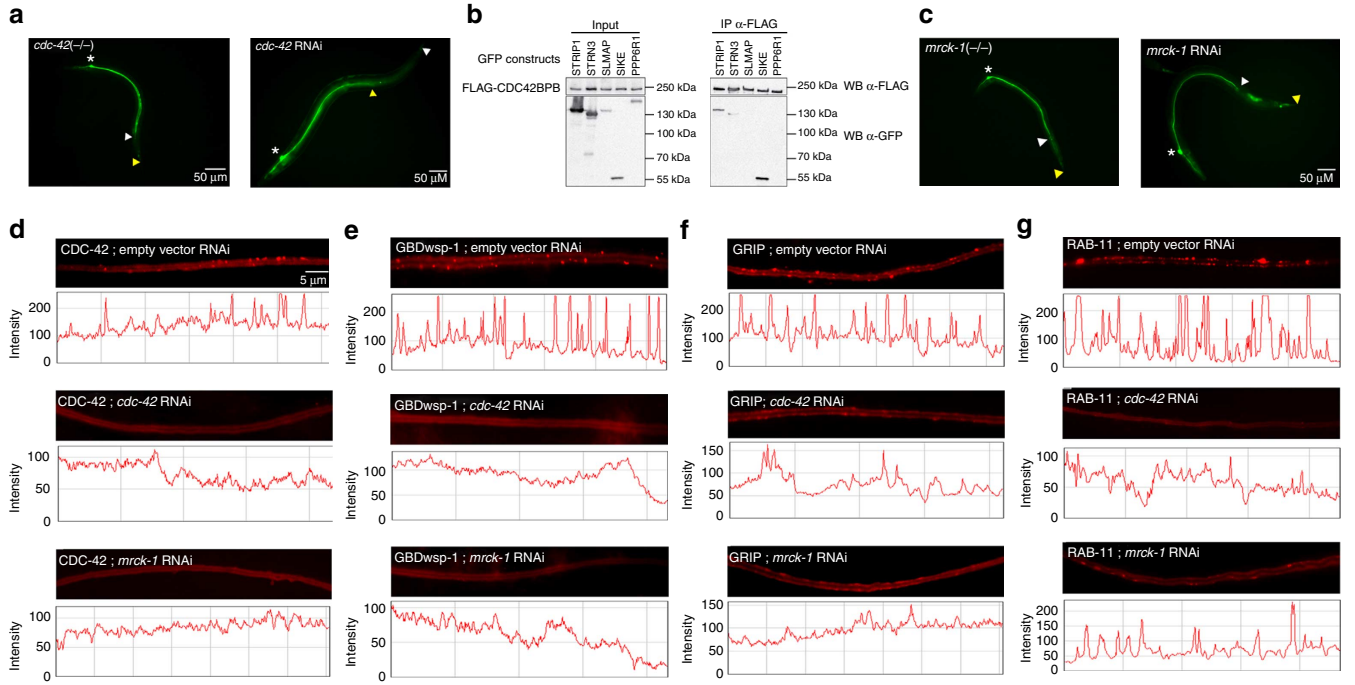

Figure 6 | CDC-42 and MRCK-1 affect canal growth and endocytic recycling. (**a**) Mutation (left) and RNAi (right) to the Rho GTPase *cdc-42* cause similar canal truncations and cysts. (**b**) CDC42BPB (aka MRCKβ) co-immunoprecipitated (**i**) with multiple STRIPAK complex components in mammalian cells. (**c**) The *C. elegans* MRCK orthologue *mrck-1* (left—mutant; right—RNA) also caused canal truncations and cysts when ablated. (**d**–**g**) RNAi to control empty vector (top), *cdc-42*(middle) and *mrck-1* (bottom), respectively. CDC-42 signalling (**d**,**e**), Golgi (**f**) and recycling endosomes (**g**) puncta are dispersed by RNAi to *cdc-42* and *mrck-1*. Asterisks denote location of the excretory cell (at the anterior/head of the worm). White and yellow arrowheads denote canal and total worm length, respectively. **a** and **c** are at × 100 magnification; **d**–**g** are at × 630 magnification. Canal sections are taken at the same region of the posterior canal, oriented from anterior (left) to posterior (right).

that CCM-3 may promote endocytic recycling, in part through effects on actin organization.

MRCK-1 is required for canal extension. Proteomic analysis of STRIPAK interacting proteins in human cells identified the CDC-42-binding protein (CDC42BPB), also known as the myotonic dystrophy-related CDC-42-binding kinase (MRCK), as another putative CCM3 interactor (J.D.R.K., M.G. and A.-C.G., unpublished data). Physical interaction between CDC-42-binding proteins and several STRIPAK components was recapitulated by immunoprecipitation coupled to immunoblotting (Fig. 6b). Given the role of MRCK in the regulation of CDC-42 signalling[46,47], which has also been reported in *C. elegans*[48], we asked whether the *C. elegans* CDC42BPB/MRCK orthologue MRCK-1 was required for canal development. Ablation of *mrck-1* by mutation or RNAi caused canal truncations and cyst formation that resembled the effect of *ccm-3*, *gck-1*, STRIPAK or *cdc-42* ablation (Fig. 6c). Similar to ablation of CCM-3, STRIPAK and CDC-42, we observed a strong dispersal of the Golgi reporter and a reduction in both REs and CDC-42/GBDwsp-1 (Fig. 6d–g, bottom panels; Supplementary Table 2). These results suggest that CCM-3 and STRIPAK promote seamless tube extension, in part through CDC-42/MRCK-1, revealing a new role for MRCK in this process.

Discussion

Elucidating how integrity of biological tubes is maintained has important implications in development, and our understanding of CCM disease, where brain capillaries develop malformations that can severely disable affected patients[16]. Our results are consistent with an emerging view that CCM3 also functions independently of CCM1 and CCM2. While the three vertebrate CCM proteins can form a ternary complex, with CCM2 acting as a hub to bind both CCM1 and CCM3 (refs 23,49,50), the apparent absence of a *CCM2* gene in *C. elegans* may explain the distinct functions of KRI-1 and CCM-3. Importantly, we show that *ccm-3* is critical for tube growth, and furthermore, that it functions by a cell-autonomous mechanism, although it is interesting to note that CCM3 can function both autonomously and non-autonomously in vertebrates[26]. The localization of CCM-3 to the apical membrane, and subsequent apical membrane defects (that is, enlarged lumen and significant accumulation of CVs in the cytoplasm), as well as frequent enrichment at the growing distal tip, reveal a conserved role for this protein in vascular tube extension and maintenance.

In mammalian cells CCM3 and its binding partners, the germinal centre kinases (MST4/STK24/STK25), are tightly associated with the STRIPAK complex and are required for Golgi polarization[25,40]. Studies in murine and fly models have suggested different roles for *CCM3* and *GCKIII* in biological tube development: promoting lumen formation in mice, and localizing junction and polarity proteins at the interface of multicellular and unicellular tubes in flies[38,51]. Growth of the terminal seamless tubes of *Drosophila* trachea are dependent on the regulation of small GTPases and vesicle trafficking, in which CCM3 and GCKIII have been implicated[51,52]. Here, we show that the *C. elegans* CCM3 and GCKIII orthologues (*ccm-3* and *gck-1*), in cooperation with STRIPAK, control seamless tube growth through CDC-42/MRCK-1-dependent regulation of endocytic recycling (Fig. 7a).

Although ablation of mammalian CCM1, -2 or -3 leads to upregulation of RhoA and ROCK[22,37,39,53], our data suggest that CCM-3 and STRIPAK preferentially modulate CDC-42

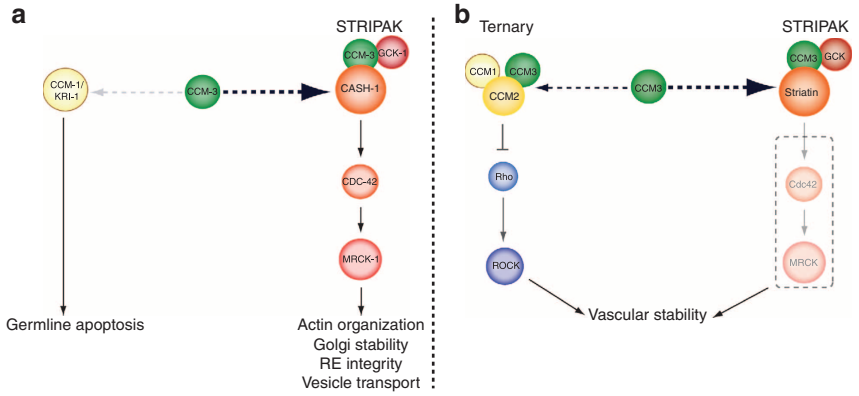

Figure 7 | Model. CCM-3/STRIPAK modulates CDC-42 signalling (ostensibly through MRCK-1) to correctly promote Golgi stability, RE integrity and vesicle transport. These roles are likely reliant on actin organization, and ultimately result in successful tube extension/maintenance. The *C. elegans* CCM-3 (**a**) acts independently of KRI-1 (in the absence of a worm CCM2 orthologue), which has no apparent role in tube development, in contrast to the vertebrate model (**b**). This may indicate a conserved role of CCM3 fundamental to biological tube development.

signalling, posing the question of whether multiple CCM3 complexes collaborate to maintain vascular stability in vertebrates. Along with recent evidence indicating that CCM3 is predominantly associated with the STRIPAK complex[40], the exceptional clinical aggressiveness caused by loss of *CCM3* could be due to synergistic defects that arise from disruption of multiple complexes. To this point, a pathological form of CCM3 found in patients, which lacks 18 amino acids in the N-terminal region, can still form a ternary complex with CCM1–CCM2 but does not bind the GCKIII kinase[53]. Since CCM3 binds both STRIPAK[25] and CCM2 (ref. 54) through its C-terminal focal adhesion kinase-targeting domain, it is possible that the two independent CCM3 complexes co-exist. Therefore, CCM3 may function in two independent pathways that regulate distinct signalling cascades through RhoA and Cdc42 to promote vascular tube development and plasma membrane stability. What we observed in *C. elegans* may represent a primitive role for CCM-3 in vasculature development that has expanded in mammals (Fig. 7).

Consistent with a role for STRIPAK in regulating GTPase signalling, we found the mammalian STRIPAK complex also interacts with the CDC-42-binding kinase MRCK. Ablation of *cdc-42* or *mrck-1* in *C. elegans* causes canal truncations similar to ablation of *ccm-3* or *gck-1*. Furthermore, punctate CDC-42 is dispersed, supressing the presence of active CDC-42 at the distal tip when *ccm-3*, *gck-1*, *mrck-1* and *cash-1* are ablated. Since we did not observe any significant canal defects after *rho-1* silencing, we favour a model in which CCM-3 and STRIPAK preferentially act through CDC-42, at least in *C. elegans*. While the mammalian CCM1–CCM2 and CCM1–CCM2–CCM3 complexes have been shown to affect Rho signalling and actin polymerization, mammalian STRIPAK proteins interact with Golgi, cytoskeletal components and proteins involved in vesicular trafficking[41]. Crucially, both complexes likely target the same process via separate signalling cascades, namely actin regulation. Given the well-established role of CDC-42 in regulating actin, and the roles of actin in Golgi shape/stability, vesicle formation, secretion and transport[13,55], we propose that CCM-3 modulates the actin cytoskeleton via CDC-42/MRCK-1 (Fig. 7a). The partial rescue of *ccm-3* mutant phenotypes by overexpression of actin supports this hypothesis, especially if loss of *ccm-3* could divert available actin pools into stress fibres.

Recent work showing differential effects on the actin cytoskeleton by ROCK and MRCK at endothelial cell junctions highlights the necessity to balance suppression of Rho/ROCK and activation of CDC-42/MRCK[56]. With excess Rho/ROCK activity, actin becomes tied up in stress fibres[22], whereas CDC-42/MRCK promotes circumferential actin bundles critical for junction formation[56]. This may explain the functional split between CCM1·CCM2·CCM3 ternary and CCM3–STRIPAK complexes in vertebrates, if the modulation of CDC-42 by CCM-3 is conserved (Fig. 7).

The apparent downregulation of endocytic recycling (reduction in RAB-11) that we observe with loss of *ccm-3* may arise through defects in Golgi integrity via the actin cytoskeleton. Indeed, Golgi-associated CDC-42 promotes vesicle formation by modulating actin polymerization[57], and is the only Rho GTPase known to regulate Golgi function[58]. Hence, where both ER and Golgi are significantly diminished in *ccm-3(−/−)* canals, defects in cytoskeleton-mediated transport of these organelles is not likely responsible since mitochondria are still present. Rather, we suspect a specific defect in Golgi (and possibly ER) stability. Fragmentation of the ER and Golgi manifests as an increased presence of vesicles[59,60], making them hard to discern from other vesicles, such as CVs. Perhaps some of the larger vesicles we detected in the EM sections of *ccm-3(−/−)* canals represent the fragmented products of ER and Golgi. Fragmentation of the Golgi may also reduce the RE integrity, which could contribute to loss of apical membrane integrity. Rab11 regulates apical REs[61,62], and its depletion in mammalian cells caused improperly localized accumulation of REs (often to the basolateral membrane), preventing functional apical recycling. This concurs with the apical phenotypes we see with loss of *rab-11*, and supports the idea that CCM-3 promotes endocytic recycling. Loss of Rab11 can also affect the exocyst complex by binding Sec15, which helps mediate communication with endocytic vesicles[44]. Both CCM-3 and the exocyst localize to the apical membrane, and the exocyst has been shown to promote lumenogenesis through vesicle fusion[45,63]. However, we are uncertain as to whether CCM-3 might act directly on the exocyst, through RAB-11, or even another protein, to affect vesicle fusion. In neutrophils, for example, CCM3 promotes exocytosis through the small GTPase Rab27 (ref. 64). In summation, it is becoming clear that CCM3 regulates multiple trafficking events, many of which are likely to be cell-type specific.

Ultrastructural analysis revealed a number of defects in the *ccm-3* mutant canal such as aggregation of CVs, ectopic lumen, abnormal lumen expansion and basolateral membrane perturbations. The basolateral perturbations, while potentially a result of defective recycling/exocytosis, are more likely due to vesicle

accumulation and radial lumen expansion. The variation in the individual CV diameter in the heavily cystic canals may reflect their nature as channels, through which hydrostatic pressure can be generated[8,9]. Expanding CVs (and possibly vesicles derived from fragmented Golgi/ER) may mechanically push the cytoplasmic contents against the membrane, causing the observed basolateral projections. The CV aggregation and enlarged lumen phenotype is particularly reminiscent of ERM-1 overexpression[8]. While there is evidence that CCM3-associated GCKIII and MRCK can phosphorylate ERM[65,66], we remain cautious of suggesting a direct interaction here, since loss of *ccm-3* did not appear to affect levels or localization of ERM-1, nor could functional ERM-1 restore full-length canals. Hence, where ERM-1 is integral to early development of the canal[8], our observations are more consistent with those of Song *et al.*[51], showing that *CCM3* defects do not prevent lumen formation *per se*, but rather lead to dilations through improper addition of membrane.

This study brings together concepts from several model systems pointing to a novel mechanism by which CCM-3, in association with STRIPAK, influences small GTPase signalling (CDC-42 and RAB-11) to maintain Golgi stability and endocytic recycling. The disease state of *CCM3* mutation is widely recognized as the most severe, and as such, we propose that CCM3 functions concurrently within two complexes to balance GTPase signalling and maintain plasma membrane stability. Our observations in the *C. elegans* excretory canal, along with mammalian conservation in CCM-3 and STRIPAK interactions, may provide insights into intrinsic mechanisms by which cavernous malformations develop in CCM patients, and help identify drug targets for alleviating or reversing CCMs.

Methods

***C. elegans* strains and maintenance.** Worms were cultivated on lawns of *Escherichia coli* (strain OP50) grown on nematode growth medium plates at 20 °C (unless otherwise stated)[67]. The following strains were provided by the *Caenorhabditis* Genetics Centre: BC13892, CF2282, RB1928, WH556 and JS345. The unbalanced *ccm-3(tm2806)/+* strain was originally obtained from the Japanese National Bioresource Project. WT refers to the *C. elegans* variety Bristol, strain N2. See Supplementary Table 5 for the strain list. All excretory canal marker strains were a kind gift from Dr Matthew Buechner. The ERM-1::GFP and ACT-5::GFP strains were a kind gift from Dr Verena Göbel.

DNA constructs and microinjection. Extra-chromosomal-rescuing arrays were generated by microinjection of a construct containing 3.2 kb of the *ccm-3* promoter and the WT *ccm-3* gene (including introns) cloned into the pCFJ151 vector, then co-injected with pCFJ90 ($P_{myo\text{-}2}$::mCherry) and pGH8 ($P_{rab\text{-}3}$::mCherry) into *ccm-3(tm2806)/mIn1* (strain WD188) worms. The *gck-1*-rescuing array was generated by isolating the WT *gck-1* gene and 1.8 kb of promoter from fosmid WRM0622bf08 and co-injected with pCFJ90 ($P_{myo\text{-}2}$::mCherry) into *gck-1(km15)/nT1* worms (strain WD195). Canal-specific rescue of *ccm-3* (strain WD382) and *gck-1* (strain WD420) was achieved by replacing the mCherry gene in pBK162 (a kind gift from Dr Matthew Buechner) with *ccm-3* complementary DNA (cDNA). The pBK162 vector contains the *exc-9* promoter to drive canal-specific expression. This rescuing plasmid was co-injected with pBK162 and pCFJ90 into *ccm-3(tm2806)/mIn1* worms (strain WD188). The CCM-3::GFP translational reporter was constructed by cloning the $P_{exc\text{-}9}$ promoter, *ccm-3* and *gfp* cDNAs into a pUC19 backbone. This construct was injected into N2, WD119 and JS345 and BK219 strains to generate strains listed in Supplementary Table 5. The GCK-1::mCherry translational reporter was constructed by cloning *gck-1* cDNA into the pBK162 vector (containing both $P_{exc\text{-}9}$ and mCherry). This construct was injected into JS345, WD119 and co-injected with the CCM-3 translational reporter into N2 worms (see Supplementary Table 5). Micro-injection was performed using a FemtoJet (Eppendorf) microinjections system attached to an inverted Leica DMI3000B microscope.

RNA interference. RNAi was performed by feeding bacteria expressing double-stranded RNA (RNAi), from the Source Bioscience LifeSciences feeding library, to worms at the L1 stage. RNAI bacteria, was streaked onto LB media plates (with ampicillin and tetracycline), and incubated for 18 h at 37 °C. Individual colonies were selected with a sterile p200 tip, and were transferred to tubes containing liquid LB + ampicillin + tetracycline. These were grown for 24 h (at 37 °C) in an orbital shaker, prior to induction with isopropyl-b-D-thiogalactoside (0.1 M) for 4 h (37 °C, orbital shaker). RNAi was plated on RNAi media plates (containing isopropyl-b-D-thiogalactoside and carbenicillin) and left to grow at room temperature overnight. Worms were staged at L1 through hypochlorite bleaching. Overgrown plates (containing many eggs) were treated with hypochlorite bleach for 5 min at room temperature, before having the bleach transferred to Eppendorf tubes. The tubes were centrifuged at 2,000 r.p.m. for 1 min and were followed by two more bleach washes/centrifugation steps and three washes/centrifugation with M9 buffer. Eppendorf tubes, containing eggs in M9 buffer, were left for 24 h in a rotary mixer (at 20 °C), and L1s were plated the following day. In the case of essential genes (such as *rab-11*), it was necessary to plate the worms on RNAi at the L3 stage.

Differential interference contrast (DIC) microscopy. L4 and young adult-staged worms were slide mounted in a 5-µl aliquot of tetramisole anaesthetic (20 mM), on a flat pad of agar (4%). Nematodes were viewed with a Leica DMRA2 compound microscope equipped with epifluorescence and Nomarski optics. The images are marked for magnification individually. Images were captured with a Hamamatsu C472-95 digital camera using Openlab software (PerkinElmer Inc.). Images reflect a single plane. Typically only a single 'arm' of the canal can be seen, with the other (in a lower plane) obscured by the intestine. The canals imaged at $\times 100$ and $\times 630$ magnification were always selected on this basis of relative clarity. Canal lengths were measured from the pharynx to the tip of the canal and were calculated relative to body length, as measured from the terminal pharynx bulb to the anus.

High-pressure freeze fixation and TEM. L4 and young adult-staged worms were fixed with high-pressure freezing, followed by freeze substitution, in a procedure modified from Stigloher *et al.*[68] A total of 10–12 worms in OP50 bacteria were transferred into the cavity of the freezing chamber (specimen carriers type A (100 µm) and B (0 µm); Bal-Tec AG, acquired by Leica Microsystems) and processed by an EM HPM100 (Leica Microsystems); freezing speed $>20{,}000\,K\,s^{-1}$, pressure $>2{,}000$ bar. The resultant frozen pellets were liberated from their carriers, directly into liquid nitrogen, to an EM AFS2 freeze substitution system (Leica Microsystems). Samples were fixed with 0.1% tannic acid and 0.5% glutaraldehyde in acetone (-90 °C for 96 h), and further washed four times for 1 h with acetone at -90 °C. The pellets were post-fixed with 2% osmium tetroxide in acetone (-90 °C for 28 h). The temperature was subsequently raised to -20 °C for 14 h, incubated for 16 h (still at -20 °C) and then raised again to 4 °C over 4 h. Pellets were washed with acetone (at 4 °C) four times at 30-min intervals. The temperature was increased to 20 °C over a period of 1 h and finally samples were embedded in a series of freshly prepared Araldite solutions. Here, concentrations increased from 50% Araldite in acetone (3 h at room temperature) to 90% Araldite in acetone (overnight at 4 °C), to pure Araldite at room temperature (two times). Araldite-treated samples were allowed to polymerize for 48 h at 60 °C. A total of 10–12 serial sections (90 nm per section) were taken at three sequential 50-µm intervals for both control (N2) and *ccm-3(tm2806)* homozygotes. Images of the excretory canal were obtained on FEI Tecnai 20 equipped with an AMT16000 digital camera.

Statistical analyses. Statistical significance of canal lengths were expressed as a percentage, and normalized to a value of 1 based on WT canals. All values in charts are mean ± s.e.m. from three or more experimental data sets. *P* values were determined using a two-tailed Student's *t*-test, assuming equal variance. Significance levels (*P* value) and sample size (*N*) are marked in each corresponding figure legend.

Puncta/fluorescent measures for endocytic/CDC-42 marker strains were conducted with Image J software using a Red, Green, Blue (RGB) profile plot on a stretch of canal (~ 100 µm in length) at or near the posterior distal tip. Each image shows a single plane, of one canal, with the maximal amount of puncta present. Relative intensity of the Red Fluorescent Protein (RFP or mCherry) was assessed, with puncta presence marked with peaks and non-punctate areas with troughs. Canal lumen volume, CV diameter and CV number measurements were conducted using ImageJ software (NIH); *ccm-3* mutant data were normalized against N2 data to show relativity.

Immunoprecipitation and immunoblotting. The mouse pcDNA3-FLAG-Mst4 (BC005708), human pcDNA3-FLAG-PPP4R2 (NM_174907) and human pcDNA5-GFP-SLMAP (BC115701) constructs used were described previously[40,69]. *C. elegans* CCM3 (NM_063889) and human PPP6R1 (BC094753) were PCR amplified from cDNA with EcoRI and NotI added at the 5′ and 3′ ends, respectively. Following digestion with EcoRI and NotI, the inserts were introduced into pcDNA5/FRT/TO-eGFP. *C. elegans gck-1* (NM_072908) was cloned similarly, except that it was inserted into pcDNA5-FLAG. Human CDC42BPB (NM_006035) in pENTR223 was obtained from the Dana-Farber/Harvard Cancer Center DNA Resource Core and recombined into pDest-pcDNA5-Flag using LR clonase. Human SIKE (BC005934), mouse Strip1 (BC023952) and human STRN3 (BC126221) were originally cloned in pcDNA3-FLAG[40]. Inserts for these genes were subsequently PCR amplified with attL1 and attL2 recombination sites added to the 5′ and 3′ ends, respectively. The PCR products were inserted into pDONR223 (Invitrogen) using BP clonase and then recombined into pcDNA5/FRT/TO-eGFP using LR clonase. All inserts were sequence verified. Immunoprecipitation and western blotting were performed as follows: low passage HEK293T cells were co-transfected using jetPRIME transfection reagent (Polyplus

Cat# CA89129-924) as per the manufacturer's protocol. Cells were lysed with 50 mM Hepes-KOH pH 8.0, 100 mM KCl, 2 mM EDTA, 0.1% NP40, 10% glycerol, 1 mM phenylmethylsulphonyl fluoride, 1 mM dithiothreitol and Sigma protease inhibitor cocktail (Cat# P8340) and subjected to passive lysis followed by one freeze–thaw cycle. Lysates were incubated with FLAG M2-agarose beads for 1.5 h, washed three times with lysis buffer and directly eluted by boiling in Laemmli buffer. Precipitated proteins were separated via SDS–polyacrylamide gel electrophoresis, transferred to nitrocellulose and detected with antibodies directed against the FLAG or GFP epitopes. These can be seen in Supplementary Fig. 9.

References

1. Lubarsky, B. & Krasnow, M. A. Tube morphogenesis: making and shaping biological tubes. *Cell* **112,** 19–28 (2003).
2. Schottenfeld-Roames, J. & Ghabrial, A. S. Osmotic regulation of seamless tube growth. *Nat. Cell Biol.* **15,** 137–139 (2013).
3. Barr, M. M. Caenorhabditis elegans as a model to study renal development and disease: sexy cilia. *J. Am. Soc. Nephrol.* **16,** 305–312 (2005).
4. Whitehead, K. J. *et al.* The cerebral cavernous malformation signaling pathway promotes vascular integrity via Rho GTPases. *Nat. Med.* **15,** 177–184 (2009).
5. Maruyama, R. & Andrew, D. J. Drosophila as a model for epithelial tube formation. *Dev. Dyn.* **241,** 119–135 (2012).
6. Buechner, M. Tubes and the single C. elegans excretory cell. *Trends Cell Biol.* **12,** 479–484 (2002).
7. Nelson, F. K. & Riddle, D. L. Functional study of the Caenorhabditis elegans secretory-excretory system using laser microsurgery. *J. Exp. Zool.* **231,** 45–56 (1984).
8. Khan, L. A. *et al.* Intracellular lumen extension requires ERM-1-dependent apical membrane expansion and AQP-8-mediated flux. *Nat. Cell Biol.* **15,** 143–156 (2013).
9. Kolotuev, I., Hyenne, V., Schwab, Y., Rodriguez, D. & Labouesse, M. A pathway for unicellular tube extension depending on the lymphatic vessel determinant Prox1 and on osmoregulation. *Nat. Cell Biol.* **15,** 157–168 (2013).
10. Mattingly, B. C. & Buechner, M. The FGD homologue EXC-5 regulates apical trafficking in C. elegans tubules. *Dev. Biol.* **359,** 59–72 (2011).
11. De Matteis, M. A. & Luini, A. Exiting the Golgi complex. *Nat. Rev. Mol. Cell Biol.* **9,** 273–284 (2008).
12. Fucini, R. V., Chen, J. L., Sharma, C., Kessels, M. M. & Stamnes, M. Golgi vesicle proteins are linked to the assembly of an actin complex defined by mAbp1. *Mol. Biol. Cell* **13,** 621–631 (2002).
13. Kroschewski, R., Hall, A. & Mellman, I. Cdc42 controls secretory and endocytic transport to the basolateral plasma membrane of MDCK cells. *Nat. Cell Biol.* **1,** 8–13 (1999).
14. Harris, K. P. & Tepass, U. Cdc42 and vesicle trafficking in polarized cells. *Traffic* **11,** 1272–1279 (2010).
15. Suzuki, N. *et al.* A putative GDP-GTP exchange factor is required for development of the excretory cell in Caenorhabditis elegans. *EMBO Rep.* **2,** 530–535 (2001).
16. Fischer, A., Zalvide, J., Faurobert, E., Albiges-Rizo, C. & Tournier-Lasserve, E. Cerebral cavernous malformations: from CCM genes to endothelial cell homeostasis. *Trends Mol. Med.* **19,** 302–308 (2013).
17. Labauge, P. *et al.* An association between autosomal dominant cerebral cavernomas and a distinctive hyperkeratotic cutaneous vascular malformation in 4 families. *Ann. Neurol.* **45,** 250–254 (1999).
18. Sahoo, T. *et al.* Mutations in the gene encoding KRIT1, a Krev-1/rap1a binding protein, cause cerebral cavernous malformations (CCM1). *Hum. Mol. Genet.* **8,** 2325–2333 (1999).
19. Liquori, C. L. *et al.* Mutations in a gene encoding a novel protein containing a phosphotyrosine-binding domain cause type 2 cerebral cavernous malformations. *Am. J. Hum. Genet.* **73,** 1459–1464 (2003).
20. Bergametti, F. *et al.* Mutations within the programmed cell death 10 gene cause cerebral cavernous malformations. *Am. J. Hum. Genet.* **76,** 42–51 (2005).
21. Guclu, B. *et al.* Mutations in apoptosis-related gene, PDCD10, cause cerebral cavernous malformation 3. *Neurosurgery* **57,** 1008–1013 (2005).
22. Stockton, R. A., Shenkar, R., Awad, I. A. & Ginsberg, M. H. Cerebral cavernous malformations proteins inhibit Rho kinase to stabilize vascular integrity. *J. Exp. Med.* **207,** 881–896 (2010).
23. Hilder, T. L. *et al.* Proteomic identification of the cerebral cavernous malformation signaling complex. *J. Proteome Res.* **6,** 4343–4355 (2007).
24. Zhu, Y. *et al.* Differential angiogenesis function of CCM2 and CCM3 in cerebral cavernous malformations. *Neurosurg. Focus* **29,** E1 (2010).
25. Kean, M. J. *et al.* Structure-function analysis of core STRIPAK proteins: a signaling complex implicated in Golgi polarization. *J. Biol. Chem.* **286,** 25065–25075 (2011).
26. Louvi, A. *et al.* Loss of cerebral cavernous malformation 3 (Ccm3) in neuroglia leads to CCM and vascular pathology. *Proc. Natl Acad. Sci. USA* **108,** 3737–3742 (2011).
27. Fidalgo, M. *et al.* CCM3/PDCD10 stabilizes GCKIII proteins to promote Golgi assembly and cell orientation. *J. Cell Sci.* **123,** 1274–1284 (2010).
28. Yoruk, B., Gillers, B. S., Chi, N. C. & Scott, I. C. Ccm3 functions in a manner distinct from Ccm1 and Ccm2 in a zebrafish model of CCM vascular disease. *Dev. Biol.* **362,** 121–131 (2012).
29. Riant, F. *et al.* CCM3 mutations are associated with early-onset cerebral hemorrhage and multiple meningiomas. *Mol. Syndromol.* **4,** 165–172 (2013).
30. Ceccarelli, D. F. *et al.* CCM3/PDCD10 heterodimerizes with germinal center kinase III (GCKIII) proteins using a mechanism analogous to CCM3 homodimerization. *J. Biol. Chem.* **286,** 25056–25064 (2011).
31. Hunt-Newbury, R. *et al.* High-throughput in vivo analysis of gene expression in Caenorhabditis elegans. *PLoS Biol.* **5,** e237 (2007).
32. Mello, C. & Fire, A. DNA transformation. *Methods Cell Biol.* **48,** 451–482 (1995).
33. Ito, S., Greiss, S., Gartner, A. & Derry, W. B. Cell-nonautonomous regulation of C. elegans germ cell death by kri-1. *Curr. Biol.* **20,** 333–338 (2010).
34. Berman, J. R. & Kenyon, C. Germ-cell loss extends C. elegans life span through regulation of DAF-16 by kri-1 and lipophilic-hormone signaling. *Cell* **124,** 1055–1068 (2006).
35. Qian, Z., Lin, C., Espinosa, R., LeBeau, M. & Rosner, M. R. Cloning and characterization of MST4, a novel Ste20-like kinase. *J. Biol. Chem.* **276,** 22439–22445 (2001).
36. Lu, T. J. *et al.* Inhibition of cell migration by autophosphorylated mammalian sterile 20-like kinase 3 (MST3) involves paxillin and protein-tyrosine phosphatase-PEST. *J. Biol. Chem.* **281,** 38405–38417 (2006).
37. Borikova, A. L. *et al.* Rho kinase inhibition rescues the endothelial cell cerebral cavernous malformation phenotype. *J. Biol. Chem.* **285,** 11760–11764 (2010).
38. Chan, A. C. *et al.* Mutations in 2 distinct genetic pathways result in cerebral cavernous malformations in mice. *J. Clin. Invest.* **121,** 1871–1881 (2011).
39. Shenkar, R. *et al.* Exceptional aggressiveness of cerebral cavernous malformation disease associated with PDCD10 mutations. *Genet. Med.* (2014).
40. Goudreault, M. *et al.* A PP2A phosphatase high density interaction network identifies a novel striatin-interacting phosphatase and kinase complex linked to the cerebral cavernous malformation 3 (CCM3) protein. *Mol. Cell. Proteomics* **8,** 157–171 (2009).
41. Hwang, J. & Pallas, D. C. STRIPAK complexes: structure, biological function, and involvement in human diseases. *Int. J. Biochem. Cell Biol.* **47,** 118–148 (2014).
42. Zhang, X. *et al.* Cdc42 interacts with the exocyst and regulates polarized secretion. *J. Biol. Chem.* **276,** 46745–46750 (2001).
43. He, B. & Guo, W. The exocyst complex in polarized exocytosis. *Curr. Opin. Cell Biol.* **21,** 537–542 (2009).
44. Takahashi, S. *et al.* Rab11 regulates exocytosis of recycling vesicles at the plasma membrane. *J. Cell Sci.* **125,** 4049–4057 (2012).
45. Armenti, S. T., Chan, E. & Nance, J. Polarized exocyst-mediated vesicle fusion directs intracellular lumenogenesis within the C. elegans excretory cell. *Dev. Biol.* **394,** 110–121 (2014).
46. Leung, T., Chen, X. Q., Tan, I., Manser, E. & Lim, L. Myotonic dystrophy kinase-related Cdc42-binding kinase acts as a Cdc42 effector in promoting cytoskeletal reorganization. *Mol. Cell. Biol.* **18,** 130–140 (1998).
47. Wilkinson, S., Paterson, H. F. & Marshall, C. J. Cdc42-MRCK and Rho-ROCK signalling cooperate in myosin phosphorylation and cell invasion. *Nat. Cell Biol.* **7,** 255–261 (2005).
48. Gally, C. *et al.* Myosin II regulation during C. elegans embryonic elongation: LET-502/ROCK, MRCK-1 and PAK-1, three kinases with different roles. *Development* **136,** 3109–3119 (2009).
49. Voss, K. *et al.* CCM3 interacts with CCM2 indicating common pathogenesis for cerebral cavernous malformations. *Neurogenetics* **8,** 249–256 (2007).
50. Stahl, S. *et al.* Novel CCM1, CCM2, and CCM3 mutations in patients with cerebral cavernous malformations: in-frame deletion in CCM2 prevents formation of a CCM1/CCM2/CCM3 protein complex. *Hum. Mutat.* **29,** 709–717 (2008).
51. Song, Y., Eng, M. & Ghabrial, A. S. Focal defects in single-celled tubes mutant for cerebral cavernous malformation 3, GCKIII, or NSF2. *Dev. Cell* **25,** 507–519 (2013).
52. Schottenfeld-Roames, J. & Ghabrial, A. S. Whacked and Rab35 polarize dynein-motor-complex-dependent seamless tube growth. *Nat. Cell Biol.* **14,** 386–393 (2012).
53. Zheng, X. *et al.* CCM3 signaling through sterile 20-like kinases plays an essential role during zebrafish cardiovascular development and cerebral cavernous malformations. *J. Clin. Invest.* **120,** 2795–2804 (2010).
54. Li, X. *et al.* Crystal structure of CCM3, a cerebral cavernous malformation protein critical for vascular integrity. *J. Biol. Chem.* **285,** 24099–24107 (2010).
55. Schuh, M. An actin-dependent mechanism for long-range vesicle transport. *Nat. Cell Biol.* **13,** 1431–1436 (2011).

56. Ando, K. *et al.* Rap1 potentiates endothelial cell junctions by spatially controlling myosin II activity and actin organization. *J. Cell Biol.* **202,** 901–916 (2013).
57. Matas, O. B., Martinez-Menarguez, J. A. & Egea, G. Association of Cdc42/N-WASP/Arp2/3 signaling pathway with Golgi membranes. *Traffic* **5,** 838–846 (2004).
58. Matas, O. B., Fritz, S., Luna, A. & Egea, G. Membrane trafficking at the ER/Golgi interface: functional implications of RhoA and Rac1. *Eur. J. Cell Biol.* **84,** 699–707 (2005).
59. Ackema, K. B., Sauder, U., Solinger, J. A. & Spang, A. The ArfGEF GBF-1 is required for ER structure, secretion and endocytic transport in C. elegans. *PloS ONE* **8,** e67076 (2013).
60. Siddhanta, A., Radulescu, A., Stankewich, M. C., Morrow, J. S. & Shields, D. Fragmentation of the Golgi apparatus. A role for beta III spectrin and synthesis of phosphatidylinositol 4,5-bisphosphate. *J. Biol. Chem.* **278,** 1957–1965 (2003).
61. Casanova, J. E. *et al.* Association of Rab25 and Rab11a with the apical recycling system of polarized Madin-Darby canine kidney cells. *Mol. Biol. Cell* **10,** 47–61 (1999).
62. Wang, X., Kumar, R., Navarre, J., Casanova, J. E. & Goldenring, J. R. Regulation of vesicle trafficking in madin-darby canine kidney cells by Rab11a and Rab25. *J. Biol. Chem.* **275,** 29138–29146 (2000).
63. Jones, T. A., Nikolova, L. S., Schjelderup, A. & Metzstein, M. M. Exocyst-mediated membrane trafficking is required for branch outgrowth in Drosophila tracheal terminal cells. *Dev. Biol.* **390,** 41–50 (2014).
64. Zhang, Y. *et al.* A network of interactions enables CCM3 and STK24 to coordinate UNC13D-driven vesicle exocytosis in neutrophils. *Dev. Cell* **27,** 215–226 (2013).
65. Nakamura, N. *et al.* Phosphorylation of ERM proteins at filopodia induced by Cdc42. *Genes cells* **5,** 571–581 (2000).
66. Fidalgo, M. *et al.* Adaptor protein cerebral cavernous malformation 3 (CCM3) mediates phosphorylation of the cytoskeletal proteins ezrin/radixin/moesin by mammalian Ste20-4 to protect cells from oxidative stress. *J. Biol. Chem.* **287,** 11556–11565 (2012).
67. Brenner, S. The genetics of Caenorhabditis elegans. *Genetics* **77,** 71–94 (1974).
68. Stigloher, C., Zhan, H., Zhen, M., Richmond, J. & Bessereau, J. L. The presynaptic dense projection of the Caenorhabditis elegans cholinergic neuromuscular junction localizes synaptic vesicles at the active zone through SYD-2/liprin and UNC-10/RIM-dependent interactions. *J. Neurosci.* **31,** 4388–4396 (2011).
69. Gingras, A. C. *et al.* A novel, evolutionarily conserved protein phosphatase complex involved in cisplatin sensitivity. *Mol. Cell. Proteomics* **4,** 1725–1740 (2005).

Acknowledgements

This work was supported by the Canadian Institutes for Health Research (MOP-123433) to A.-C.G. and W.B.D., and a generous donation from Angioma Alliance Canada and CCM3 Action to W.B.D. A.-C.G. is the Canada Research Chair in Functional Proteomics and the Lea Reichmann Chair in Cancer Proteomics. B.L. was supported by a fellowship from the Excellence in Radiation Research for the 21st Century (EIRR21) research training program, through the CIHR. J.D.R.K. was supported by a postdoctoral fellowship from the Canadian Heart and Stroke Foundation. We thank Matthew Buechner and Verena Göbel for strains and expression vectors, Stuti Bhandari for assistance in RNAi screening and Valeriya Laskova for help with EM techniques. We are grateful to Geoffrey Hesketh and Julie Brill for comments on the manuscript.

Author contributions

B.L. performed experiments, analysed and assembled most of the data, contributed to project design and wrote the manuscript. B.Y. contributed to the generation of transgenic strains and performed all microinjections. P.X., L.Z., K.C. and E.W. generated transgenic strains, performed RNAi experiments and made canal measurements. D.H. and B.L. performed the HPF TEM and analyses, with further contributions from M.Z. and B.Y. M.G. and J.D.R.K. performed mammalian cell experiments, directed by A.-C.G. W.B.D. conceived and directed the project, participated in experiments and manuscript writing.

Additional information

Supplementary Information accompanies this paper at http://www.nature.com/naturecommunications

Competing financial interests: The authors declare no competing financial interests.

Reprints and permission information is available online at http://npg.nature.com/reprintsandpermissions/

How to cite this article: Lant, B. *et al.* CCM-3/STRIPAK promotes seamless tube extension through endocytic recycling. *Nat. Commun.* 6:6449 doi: 10.1038/ncomms7449 (2015).